Title
DIFFUSION INDUCED DEFECTS IN TRANSISTORS - PART II

Authors
Levine, E.
Thomas, G.
Washburn, J.

Publication Date
1966-05-01

UCRL-16895

University of California

Ernest O. Lawrence Radiation Laboratory

DIFFUSION-INDUCED DEFECTS IN TRANSISTORS - PART II

Berkeley, California

Submitted to Journal of Applied Physics UCRL-16895

UNIVERSITY OF CALIFORNIA
Lawrence Radiation Laboratory
Berkeley, California

AEC Contract W-7405-eng-48

DIFFUSION INDUCED DEFECTS IN TRANSISTORS - PART II

E. Levine, G. Thomas and J. Washburn

May 1966

UCRL-16895

DIFFUSION INDUCED DEFECTS IN TRANSISTORS - PART II

E. Levine, J. Washburn and G. Thomas

Inorganic Materials Research Division, Lawrence Radiation Laboratory, and Department of Mineral Technology, College of Engineering, University of California, Berkeley, California

ABSTRACT

The defect substructure produced by a double diffusion of boron and phosphorus into a silicon wafer has been studied by transmission electron microscopy. Specimens were examined at all stages in the diffusion and at all important levels in the final npn transistor wafer for both {111} and {110} oriented wafers. Similar specimens in the {112} orientation were examined at the emitter surface only.

Diffusion induced dislocations and precipitates were observed at the emitter surface in all orientations. No defects were found at other levels in the doubly diffused wafers except for {110} foils in which long dislocations capable of glide on the inclined {111} planes were observed at the emitter base junction.

The precipitates were in the form of thin platelets which produced displacement fringes parallel to their intersection with the surface ($\bar{g}.\bar{R}$ contrast) and parallel moiré fringe contrast. In addition they were strongly attacked by both HF and HNO_3 solutions. Diffraction

patterns from the precipitates were indexed as from a base centered orthorhombic structure with a = 6.3Å, b = 3.8Å and c = 6.75Å. The orientation relationship with the silicon matrix was [111]Si // [011]p. The thin platelets appeared to be a partially coherent precipitate with an associated misfit vector of ~1/3 [111] such that the platelets compressively stressed the matrix. This compressive stress acts to partially relieve the diffusion induced tensile stress normal to the habit plane, and so the operating planes are those which are most perpendicular to the diffusion front so as to have the greatest possible resolved compressive stress in the diffusion front.

I. INTRODUCTION

Diffusion into the surface layers of silicon using solutes with smaller atomic radii than that of the host silicon atom results in a solute contraction stress and the generation of an array of dislocations. This array moves deeper in the diffused wafer along with the diffusion front.

The dislocation arrays have been studied in detail for single diffusion of boron or phosphorus into {111} and {100} [1,2,3] oriented wafers, and for a double diffusion into {110} oriented wafers.[2] Arrays of edge dislocations are observed that move into the crystal along with the diffusion front by both climb and glide motions. Climb appears to predominate for {111} wafers, whereas glide is the more important motion in the {100} wafers. Diffusion into {110} wafers appears to be an intermediate case with both climb and glide operative.

In addition to dislocation arrays, precipitation is frequently observed in singly diffused structures.[2,4] Tannenbaum[5] has shown that with high concentrations of phosphorus there is a significant difference between the solute profile determined by sheet resistivity and that by radioactive tracer analysis. This could be explained by precipitation. Schmidt and Stickler[4] have made electron microscope observations of precipitates in a phosphorus diffused sample and have reported their crystal structure and orientation dependence. Doubly diffused wafers in which both phosphorus and boron are introduced at a surface are widely used in industry to produce npn transistors. Any defects that are introduced by the diffusion treatment may lead to inferior electrical properties. It is therefore of interest to investigate the devects introduced by double diffusion.

It is the purpose of the present paper to characterize the defect substructure that occurs at various levels in an npn double diffused silicon wafer and to amplify the results given in part I.[2] The main emphasis will be on the characteristics of precipitation in such wafers but observations on the dislocation content at various levels in a {111} oriented transistor wafer will also be reported.

II. EXPERIMENTAL

Silicon wafers of {111}, {112} and {110} orientation were prepared for diffusion as described in Part I. The wafers were symmetrically diffused from both sides in an open tube configuration furnace and air cooled from the diffusion temperature. Electron microscope foils were prepared according to the following procedure: A p layer was formed by a boron diffusion treatment, (B_2H_6 source for 30 minutes at 1050°C). The sample was then divided in half and foils for transmission electron microscopy were prepared at the surface (a) and at the pn junction exposed by anodic sectioning of the p layer (b) (see Fig. 1a). A second wafer which was given the same boron diffusion was then given a phosphorus diffusion, (P_2O_5 source at 1000°C for 15 minutes). This sample was divided into 3 sections. Foils for electron microscopy were obtained at three different levels as shown in Fig. 1b): 1) the emitter surface, c, 2) the emitter base junction, d, 3) the base collector junction, e. The preparation of foils for electron microscopy was done as described previously.[6] Before the thinning operation, some diffused wafers were cleaned by boiling in a concentrated nitric acid solution and rinsed in hydrofluoric acid and distilled water. Other specimens were cleaned with only a HF rinse.

Burgers vectors of dislocations and stereopair images were obtained as described in Part I. Foil orientations were found by comparison to a Kikuchi Map.[7]

III. RESULTS AND DISCUSSION

A. {111} Wafers

For {111} wafers only the emitter surface after double diffusion (foil c) contained observable defects. Dislocations introduced by the boron diffusion would not appear in any of these specimens because as shown in Part I they exist at a depth about 2/3 the distance to the p-n junction.

The density of phosphorus induced dislocations observed near the surface was $10^9/cm^2$ which is similar to that reported by Joshi and Wilhelm.[(3)] A stereo pair of a typical area is shown in Fig. 2.
The diffusion temperature was much lower than that of Joshi and Wilhelm, 3
i.e., 1000°C compared to 1150°C, yet the density of dislocations was equal or higher than they observed.

All Burgers vectors of dislocations found in these {111} phosphorus diffused samples were in the {111} plane which was parallel to the diffusion front. The directions of the dislocations meeting at a given node were usually <112> or its projection in the foil plane, i.e. edge orientations. Noticeable in the background of Fig. 2 and aligned in the three <110> directions are elongated black-white images. The apparent precipitation giving rise to these images produced no effect on the diffraction pattern. The precipitate images were useful in the interpretation of the dislocation array because they marked the original surface and therefore the direction of diffusion. In Fig. 2 most of the dislocations are located nearer the chemically polished surface except for the their ends which in many cases extend to the original surface of the wafer. Burgers vectors of most of the dislocation segments are easily recognized because they are usually in the ⟨110⟩ direction that is most nearly perpendicular to the line and parallel to one of the precipitate images. The network is three dimensional and, as was the case for single phosphorus diffusion into {111} wafers, appears to have moved into the crystal primarily by climb.[2]

Figure 3, which was obtained near an edge, clarifies the nature of the precipitate images in this foil. All three sets of precipitates are in contrast although $\bar{g}$ is parallel to one family. They are sometimes lighter and sometimes darker than background. This would be expected if the contrast arose from a local change in thickness of the foil associated with the precipitate. That this is the nature of the contrast in the thin regions is verified by the thickness contours observed along the right edge. Following the second and third contour, from the edge, in area A of Fig. 3 it is observed that they jut forward into a v shape on reaching the precipitate. This indicates that in order to maintain constant thickness the contour must move further into the foil and thus the "precipitate" is in reality an etched-out groove. The maximum depth can be approximately obtained by assuming a constant thickness change between the second and third extinction contour. The calculated extinction distance for the {220} beam is approximately 600Å. Thus the thickness at contour two is 1200Å and at three is approximately 1800Å. The second contour on reaching the precipitate juts into the foil at half the distance to the third contour. Thus at this position the thickness is 1500Å away from the cavity and 1200Å at the cavity and the depth of the cavity is approximately 300Å. The foil is approximately 3300Å thick in this region. Thus at this cavity there is a 9% decrease in thickness. The images are thus not due to precipitates but to cavities left where precipitates have been etched away. This result is confirmed by dark field strain contrast imaging.

The precipitates in this specimen were assumed to have been removed during the cleaning operation, leaving only a groove. The fact that no precipitate reflections were ever observed suggests that the amount of remaining precipitate, if any, was extremely small.

To avoid losing the precipitates a similar specimen was prepared and examined after cleaning only in cold HF. Precipitation was observed at the doubly diffused surface as shown in Fig. 4. Fringe contrast parallel to the intersection of the precipitate with the surface is visible. Tilting experiments showed that the precipitation occurred as sheets parallel to the three ⟨111⟩ planes at 70° to the foil surface, thus their traces are in the ⟨110⟩ direction in the (111) plane of observation.

Diffraction patterns from edge-on precipitates were obtained with the silicon matrix in a (112) and (011) orientation. The specimen was tilted about the $[11\bar{1}]$ axis between these two orientations. The resultant diffraction patterns, Fig. 5a, b, c, consisted of the matrix spots from a (112) and (011) oriented silicon specimen with superimposed precipitate reflections, and multiple diffraction spots. The double diffraction effects are manifested as an array of spots around the main precipitate reflections. This array is altered in sequence as shown in Fig. 5b and c when the specimen is tilted slightly to bring different matrix reflections onto the reflecting sphere. The complete pattern of spots is produced by considering each of the strong matrix reflections to act in turn as a primary beam.

The diffraction patterns from these foils taken for identical orientation but at different areas sometimes contained reflections that were not explained, suggesting that more than one precipitate may have been present. The indexed reflections represent those that consistently appeared in many diffraction patterns corresponding to different areas in the same orientation. The diffuseness of the precipitate spots decreased the accuracy of the d spacing measurements.

The precipitate reflections in Fig. 5a, b were tentatively indexed as arising from a base centered orthorhombic structure with $a = 6.3\text{Å}$, $b = 3.8\text{Å}$ and $c = 6.75\text{Å}$. The orientation relationship with the silicon matrix is $[111]\ Si$ // $[001]_p$ and $[110]_{Si}$ // $[010]_p$. These observed precipitate relationships and lattice constants differ from those reported for silicon phosphide.[4] The precipitate may be a modification or complex of silicon phosphide due to the prediffusion of boron and the presence of oxygen. Strains are minimized when the precipitate grows as a thin plate with the maximum misfit in a direction perpendicular to the plate while the habit plane of the precipitate is relatively undistorted. A positive misfit occurs in the <111> direction and thus the strain field surrounding a precipitate plate is similar to that of an extrinsic Frank dislocation half loop.

Parallel moiré fringes were also observed superimposed on the precipitate images as shown in Fig. 6. The orientation is near (112) and the precipitates in which the moire fringes were observed are perpendicular to the foil plane. The moire images are parallel to the trace of the $(11\bar{1})$ plane. The observed spacing (42Å) agrees quite well with the calculated value of 46Å using $|\bar{g}_{11\bar{1}} Si|^{-1} = 3.14$Å and $|\bar{g}_{002p}|^{-1} = 3.37$Å. The fact that these moiré patterns were observed when the precipitate was perpendicular to the plane of the foil indicates that either a non uniform thickening has occurred on at least some of the precipitates or that growth occurred along the oxide-silicon interface as well as on the {111} planes. A possible example of precipitation lying at this interface may be seen in Fig. 4 at B where moiré fringes on the (111) plane were observed.

From the diffraction evidence it is impossible to conclusively identify the precipitates; however, they do not appear to be similar to the SiP observed by Schmidt and Stickler.[4]

In Fig. 4 the precipitates appear to be making an important contribution to the relief of the diffusion induced tensile stresses because the only dislocations near a precipitate are those at right angles with a Burgers vector parallel to the precipitate. Dislocations of this type relax the stresses in the direction parallel to the precipitate. The precipitate relaxes the diffusion induced stress in the direction parallel to the dislocation lines. The effective Burgers vector of the precipitate is in the <111> direction perpendicular to the platelet, which is the direction of greatest misfit with the silicon matrix.

A large component of this misfit lies in the plane of diffusion, due to the 70° inclination of the {111} planes.

B. (112) Wafers

Electron microscope specimens were also obtained from a (112) oriented wafer prepared similarly to the (111) wafer described above. The resulting emitter surface is shown in Fig. 7. The diffraction patterns were similar to those in Fig. 5a. The precipitation is completely confined to the $(11\bar{1})$ plane perpendicular to the diffusion front. Precipitation on these perpendicular {111} planes would most effectively relieve the diffusion induced lattice contraction stress because the misfit vector of the platelets lies in the (112) plane. The only dislocations observed were those lying along the $[11\bar{1}]$ direction with Burgers vectors parallel to the trace of the precipitate platelets, i.e. $[1\bar{1}0]$. No dislocations with inclined Burgers vectors were observed; the biaxial tension stresses being relaxed in one direction by the precipitate platelets and in the second direction by the single set of edge dislocations. The solute contraction stress developes during the diffusion treatment. Therefore, the precipitate platelets must have formed at the diffusion temperature.

The morphology of the precipitates and the dislocation arrangement near precipitates in both {111} and {112} specimens shows clearly that the stress field around precipitates is compressive.

Similar to the results obtained in {111} oriented foils, no visible defect structure was observed at specimen levels a and b (Fig. 1). As reported in Part I, sample 2c contained a network of dislocations, some of whose Burgers vectors lay in the inclined {111} planes. Examination of level d showed that these glide dislocations had penetrated to the emitter base junction. No defects were observed at level e (see Fig. 1ii).

Level c also contained precipitation which was identical to that observed in the {111} and {112} oriented foils. The diffused wafers were subjected to a cleaning treatment before chemical thinning similar to the {111} foils (i.e. HNO_3 and HF). The resulting thin foils had a much lower density of precipitation than that in uncleaned foils. Also the distortion of the foil surface was considerably reduced and thus more detailed observations could be carried out on the precipitates. The observed precipitation, as expected, was confined mainly to the perpendicular {111} planes.

The precipitates were not distributed on a homogeneous scale throughout the foil but were confined to small areas separated by areas of high dislocation population as can be seen in Figs. 10, 11 and 12. The area around a patch of precipitates usually had very few dislocations.

C. <u>{110} Wafers</u>

For the {110} orientation solute contraction stresses can be relieved in both directions by growth of precipitates on the two planes perpendicular to the surface. This may explain the absence of dislocations near the precipitates for this orientation. Precipitation was not distributed homogeneously but rather was clustered as shown in Figs. 8, 9, 10. Figure 9a and b respectively show the precipitate images for a near (110) orientation and after 12° tilt about the [1$\bar{1}$0] direction. The precipitates on the perpendicular (111) planes have a semieliptical plate like shape and as at A in 9b are beginning to show fringe contrast.

The lighter than background areas apparent in Figs. 8 and 9 are caused by a preferential attack by the polishing solution near the precipitate cluster. The stereo pair in Part I, Fig. 7, showed clearly that the pit and precipitates were on opposite surfaces of the foil. This suggests that below the regions where a precipitate cluster forms there is a region of different composition, probably a region of lower phosphorus concentration. This causes a preferential attack by the chemical polishing agent even before the deepest precipitate plate was reached during polishing from the back side. The extreme "patchy" occurrence of precipitation further suggests that local fluctuations in composition existed near the oxide surface during the diffusion process.

A thin foil with areas of precipitation similar to that shown in Fig. 10 was placed in a concentrated hydrofluoric acid solution for approximately 20 sec. Hydrofluoric acid does not attack silicon but will remove any phosphides or oxides that are present. After this cleaning treatment the foil was re-examined in the electron microscope. It now contained many areas similar to that shown in Fig. 10 which were leached out during the acid treatment (Fig. 11). One can also see in Fig. 11 at A that part of one defect is still remaining. Only the thicker portion appears to have been dissolved by the cleaning treatment. The contrast at A (Fig. 11b) from the remaining part of the defect is similar to that which would be expected from an interstitial Frank dislocation half loop lying in a {111} plane perpendicular to the plane of the foil, i.e. $\bar{g}.\bar{b}=1$. Shockley partials would not be visible for the reflection used.[12]

Since most of the precipitation occurred on the perpendicular {111} planes it was difficult to further investigate the nature of the precipitate in this orientation because of the small tilt possible in the microscope (~20° max). Consequently foils were wedged in the holder so as to observe precipitates on the $(\bar{1}11)$ and $(1\bar{1}1)$ planes at a more favorable angle. The exact orientation of the foil after wedging could not be preselected but a rapid determination of the orientation could be made by comparison with Kikuchi Maps for silicon.[7]

Examination of a {110} diffused foil, tilted into the (112) orientation showed that the platelets exhibited fringe contrast similar to that of stacking faults and to that of the precipitates seen in {111} foils (see Fig. 12). The pair of micrographs 13a and b shows that the precipitate is bounded by a dislocation (Fig. 13a) which is out of contrast in Fig. 13b. The fringe contrast, however, is still visible. Using a $3\bar{1}\bar{1}$ reflection the fringe contrast was invisible but the surrounding dislocation was in contrast.

Silcock and Tunstall[13] have recently shown that for large deviations from the Bragg angle, contrast effects that cannot be accounted for by using a simple $\bar{g}.\bar{b}$ criterion are observed. They can be accounted for, however, by considering the term $[\bar{g}.\bar{b}x\bar{u}]$ in the equations devised for the dynamical theory of contrast, (where $\bar{u}$ is a unit vector tangent to the dislocation line). These authors found, however, that when $g.b \neq 0$ this term did not appreciably affect the intensity of the dislocation image. In our work deductions concerning the Burgers vector of imperfect dislocations were made in dark field at $s = 0$ and for all of the reflections used $g.b \neq 0$. Thus, both difficulties pointed out by Silcock and Tunstall [13] were avoided and the contrast was deduced using the simple criterion for partials that when $g.b = \pm 1/3$ they are invisible, but when $g.b \geq 2/3$ partials are visible.

The plane of the defect in Fig. 13 is $(1\bar{1}1)$*. Assuming the usual displacement vectors associated with stacking faults, the $\bar{g}.\bar{b}$ products for possible partial dislocations on this plane are shown in Table I.

According to the criteria of Table I the fault should be out of contrast for the $3\bar{1}\bar{1}$ reflection, based on a simple stacking fault model (that is when $\bar{g}.\bar{b}$ is integral). This is what was observed. Since the dislocation is in contrast for both the $2\bar{2}0$ and $3\bar{1}\bar{1}$ reflections it could be either a Frank partial $b = a/3\ [1\bar{1}1]$ or a Shockley partial of $\bar{b} = a/6\ [\bar{1}12]$ type. However, from the observed contrast of the end-on defect (A in Fig. 12) the partial cannot be a Shockley. Under contrast experiments, all of the defects of the $(1\bar{1}1)$ plane in Fig. 11 behaved similarly to the defect in Fig. 13 and thus are identical in nature. To further substantiate that the dislocations bounding the precipitates were pure edge dislocations, contrast experiments were done utilizing the

---

*The unique habit plane is immediately deduced from the unique orientation obtained by Kikuchi and trace analysis.

reflections indicated in Table II. This analysis was facilitated with the aid of the [001] Kikuchi Map.

In all cases the boundary dislocations behaved as Frank partials. The nature of the fault contrast, i.e., whether extrinsic or intrinsic, was determined using both the methods outlined by Bell et al.[8] and by Gevers et al.[14] Both techniques showed that the contrast was extrinsic or interstitial.

In a few cases a dislocation lying in the (110) plane appeared to be associated with one of the longer precipitates on the perpendicular {111} planes. In Fig 14, a dislocation of Burgers vector $\frac{a}{2}$ $[1\bar{1}0]$ appears to have provided the nucleus for growth of the long precipitate on the $(\bar{1}11)$ plane.

SUMMARY AND CONCLUSIONS

The precipitates are in the form of thin platelets with a bounding Frank Dislocation and they lie predominantly on the {111} planes that are most nearly perpendicular to the surface. The maximum misfit is in the c direction, which is perpendicular to the plane of the platelet. The diffraction contrast has been found to be consistent with an extrinsic fault with a normal displacement vector in $[1\bar{1}1]$. However, the magnitude of the displacement vector for a given platelet may not be exactly 1/3 ⟨111⟩. A small deviation from this value would result in the observed contrast. Since the diffusion induced stress is tensile, these second phase platelets act to reduce this stress.

The form of the precipitate strongly suggests a similar mechanism to that proposed by Booker and Tunstall for the growth of oxide plates in silicon.[15] The precipitation in its early stage of growth may be similar to an extrinsic stacking fault as one layer of precipitate with a layer repeat distance of 6.75Å would correspond to two layers of silicon with a 3.18Å repeat distance. If further thickening of the platelet occurs such as is indicated in Fig. 6 and the partially dissolved platelet in Fig. 11b the strain in the system may be relieved by removing one or more planes of atoms parallel to the habit plane of the precipitate. Thus, the platelet may become a sink for vacancies.[16] The precipitates are in the form of three plates parallel to {111} of the matrix and are probably base centered orthorhombic with $\langle 001 \rangle_p // \langle 111 \rangle_{si}$.

Thus, the results herein have shown that massive precipitation occurs in the surface layers of a doubly diffused structure during the phosphorus diffusion treatment. The growth plane of the precipitate is controlled by the diffusion induced stresses. The fact that the precipitates do not extend into the junction indicates that it probably does not directly affect junction properties.

Previous authors have inferred by etch-pit sutdies that penetration of the junction by dislocations occur. In this study, dislocations penetrated to the emitter-base junction in only $\langle 110 \rangle$ foils in which dislocations capable of glide into the wafer are created as part of the basic network.

ACKNOWLEDGEMENTS

We should like to thank ITT Shockley Laboratory of Palo Alto and Paul Van Loon for performing the diffusion and sectioning of the silicon wafers.

The continued financial support of the United States Atomic Energy Commision is gratefully acknowledged.

REFERENCES

1. J. Washburn, G. Thomas and H. J. Queisser, J. Appl. Phys., 35, 1909 (1964).
2. E. Levine, J. Washburn, G. Thomas, Part I, J. Appl. Phys., to be published.
3. M. L. Joshi and F. Wilhelm, J. Electrochem. Soc., 112, 185 (1965).
4. P. F. Schmidt and R. Stickler, J. Electrochem. Soc., 111, 1188 (1964).
5. E. Tannenbaum, Solid State Elect., 2, 123 (1961).
6. R. H. Finch, H. J. Queisser, G. Thomas, J. Washburn, J. Appl. Phys., 34, 406 (1963).
7. E. Levine, W. L. Bell, G. Thomas, J. Appl. Phys., 37, 2141 (1966).
8. W. L. Bell and G. Thomas, Phys. Stat. Solidi, 12, 843 (1965).
9. M. F. Ashby and L. M. Brown, Phil. Mag., 8, 1649 (1963).
10. M. Ruhle, M. Wilkens and U. Essmann, Phys. Stat. Solidi, 11, 819 (1965).
11. E. S. Meieran and I. Blech, Bull. Am. Phys. Soc., Abstracts, 11, 402 (1966).
12. G. R. Booker, Discussions Faraday Soc., 5118 (1964).
13. J. Silcock and W. Tunstall, Phil. Mag., 361 (1964).
14. R. Gevers, A. Art and S. Amelinckx, Phys. Stat. Solidi, 9, 1563 (1963).
15. G. Booker and W. J. Tunstall, Phil. Mag., 13, 71 (1966).
16. R. G. Baker, D. G. Brandon and J. Nutting, Phil. Mag., 4, 1339 (1959).

FIGURE CAPTIONS

Fig. 1 Schematic of specimen preparation with level examined in microscope indicated by arrow. (a-e)

(i) diffusion of boron to produce emitter

(ii) doubly diffused wafer

Fig. 2 Stereo pair of diffusion induced dislocations found at emitter surface (level iic). Three families of precipitates can be seen, lying near the original diffusion surface. NOTE - hold stero glasses approximately 6" above and centered on the picture which should be well lighted. Rotate glasses until the black dots in the center of each picture are superimposed.

Fig. 3 Thickness contours near edge of silicon sample containing apparent precipitates. The behavior of the contours at the "precipitate" A is characteristic of a cavity 300Å deep.

Fig. 4 Precipitation at emitter surface in (111) doubly diffused transistor. The foil is in exact [111] orientation and the platelets are parallel to ⟨110⟩ directions. The dislocations lie along the ⟨112⟩ direction which is perpendicular to the precipitate trace and are of pure edge type. These dislocations partially relieve the diffusion induced stress parallel to the precipitate whilst the precipitate relieves the stress in the direction parallel to the dislocation.

Fig. 5 Diffraction patterns from edge-on precipitate.

(a) Silicon matrix in (112) orientation

(b,c) Silicon matrix in (011) orientation with different strong matrix reflections operating. Note the alternation in the multiple diffracted spots.

Fig. 6 Parallel moiré fringes can be observed superimposed on the precipitates. The orientation is near (112) and the precipitates in which the moiré fringes are observed are perpendicular to the foil plane.

Fig. 7 Diffusion induced defects at the emitter surface of a (112) wafer. The foil is in symmetrical (112) orientation. Only one type of dislocation was observed, e.g., one whose Burgers vector is parallel to the precipitate. The precipitate relieves the stress in the $[11\bar{1}]$ direction.

Fig. 8 Precipitation at emitter surface in a (110) doubly diffused structure. Preferential etching has occurred in the vicinity of the precipitates.

Fig. 9 Typical area of foil showing precipitation on perpendicular (111) planes with the surrounding area having been preferentially dissolved.

(a) near (110) orientation

(b) after 12° tilt about $\bar{1}10$ axis. Note the semielliptical shape of the precipitates. At A, displacement fringes are visible.

Fig. 10 Precipitation at emitter surface in [110] doubly diffused wafer. Precipitates appeared in very dense patches of plates on the perpendicular (111) planes. Frequently as at A above, thickening appears to have occurred over only part of the platelet. A few precipitates on the less steeply inclined planes are apparent in this micrograph (b) but their form appears to be more hexagonal in shape.

Fig. 11 Typical area of foil after rinsing in cold HF solution

(a) leached out areas which prior to the acid treatment contained precipitation similar to that shown in Fig. 12.

(b) Contrast at defect in Area A, part of which has been dissolved by the acid.

Fig. 12 Precipitates after wedging [110] diffused wafer into (112) orientation. Displacement fringes are associated with the precipitates lying on the $1\bar{1}1$ planes. The bounding dislocation is out of contrast for the reflection used.

Fig. 13 Precipitate contrast in wedged orientation (near 112)).

(a) Defect shows both fringe contrast and dislocation contrast.

(b) Defect shows fringe contrast only.

Fig. 14 A dislocation of $a/2\ [1\bar{1}0]$ Burgers vector which appears to be associated with a fault on the $(\bar{1}11)$ plane. The fault which formed from this dislocation extends into an area of dense precipitation.

TABLE I

Contrast conditions (i.e. $\bar{g}.\bar{b}$ values) for partial dislocations in $(1\bar{1}1)$.

Dislocation/reflection	$\bar{1}\bar{1}1$	$2\bar{2}0$	$3\bar{1}\bar{1}$
1/6 $[\bar{1}12]$	1/3	-2/3	-1
1/6 [121]	-1/3	-1/3	0
1/6 $[21\bar{1}]$	-2/3	1/3	1
1/3 $[1\bar{1}1]$	1/3	4/3	1

TABLE II

Contrast Conditions for defects on $(1\bar{1}1)$

Defect on $(1\bar{1}1)$	Reflections 400	$\bar{1}3\bar{1}$	$31\bar{1}$	$13\bar{1}$
1/6 $[21\bar{1}]$	4/3	1/3	4/3	1
1/6 $[\bar{1}12]$	-2/3	1/3	-2/3	0
1/6 [121]	2/3	2/3	2/3	1
1/3 $[1\bar{1}1]$	4/3	-5/3	1/3	-1
Dislocation contrast	in	in	out	in
Fault Contrast	"	"	in	out

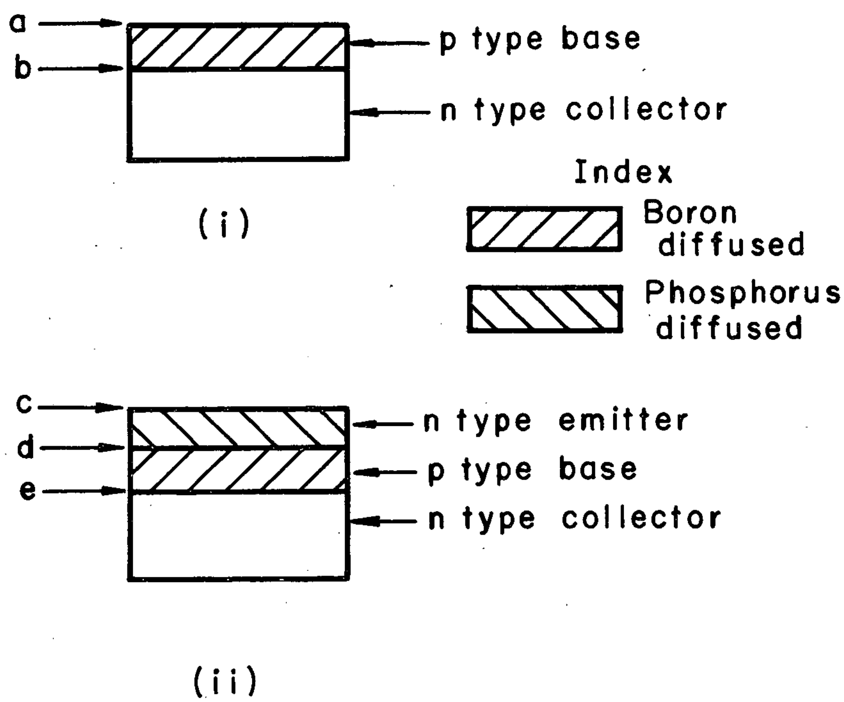

MUB-11076

Fig. 1

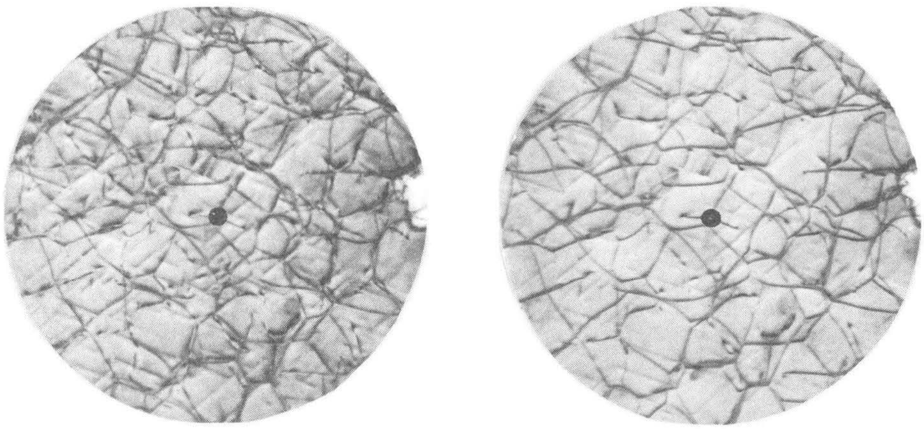

ZN-5695

Fig. 2

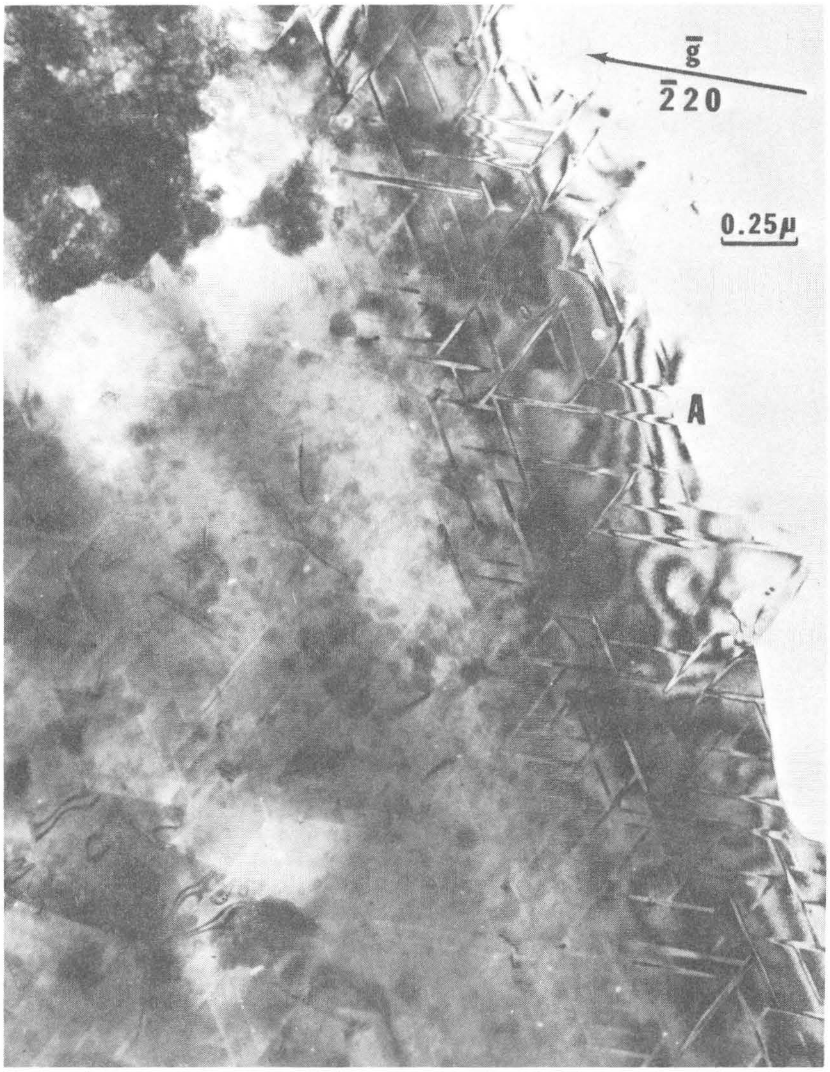

ZN-5662

Fig. 3

ZN-5663

Fig. 4

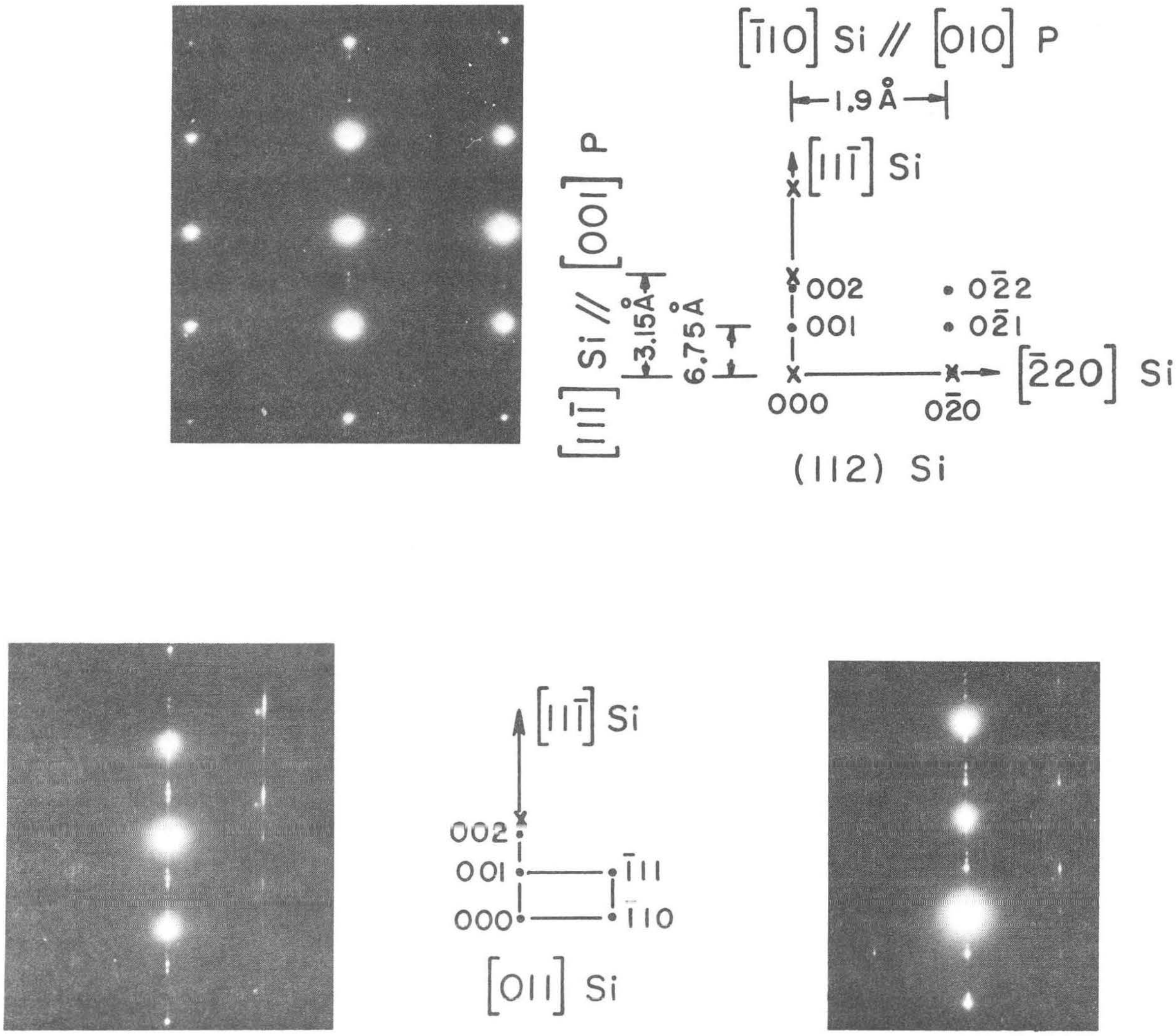
$[\bar{1}10]$ Si // [010] P
1.9 Å
$[11\bar{1}]$ Si
002
$0\bar{2}2$
001
$0\bar{2}1$
$[11\bar{1}]$ Si // [001] P
3.15 Å
6.75 Å
000
$0\bar{2}0$
$[\bar{2}20]$ Si
(112) Si
$[11\bar{1}]$ Si
002
001
$\bar{1}11$
000
$\bar{1}10$
[011] Si

ZN-5660

Fig. 5

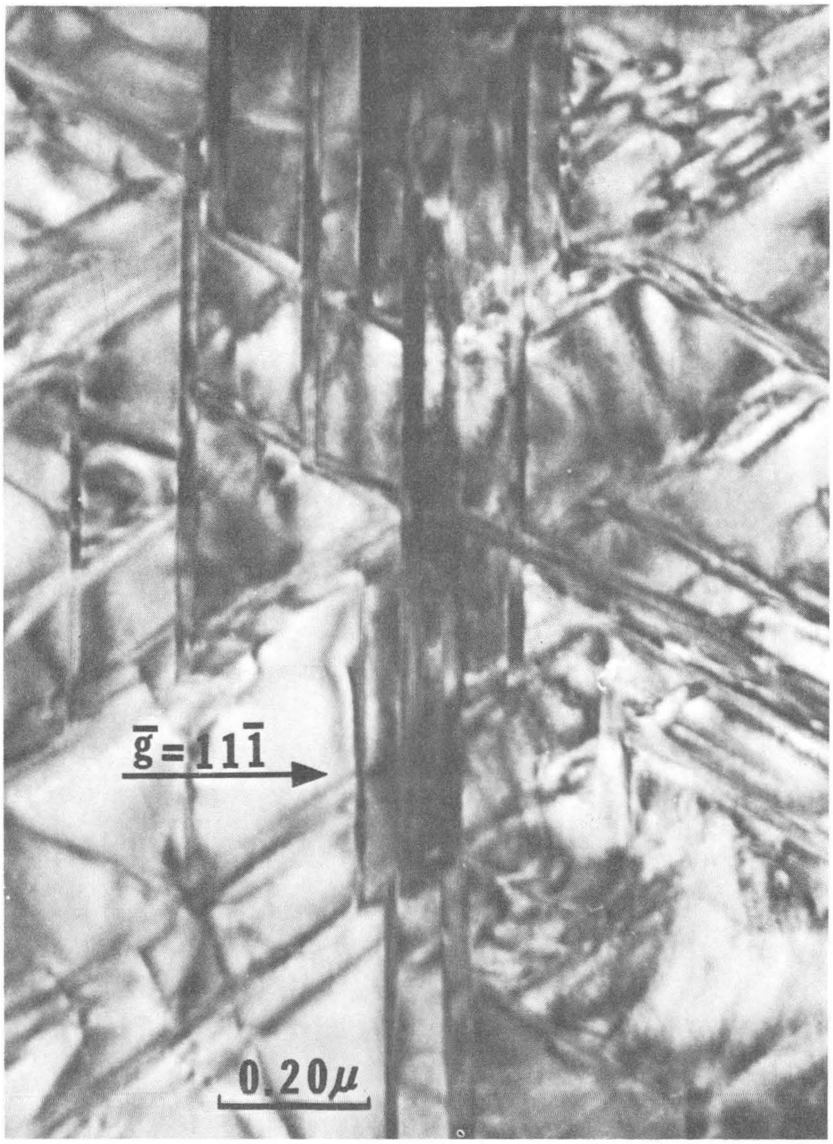

ZN-5661

Fig. 6

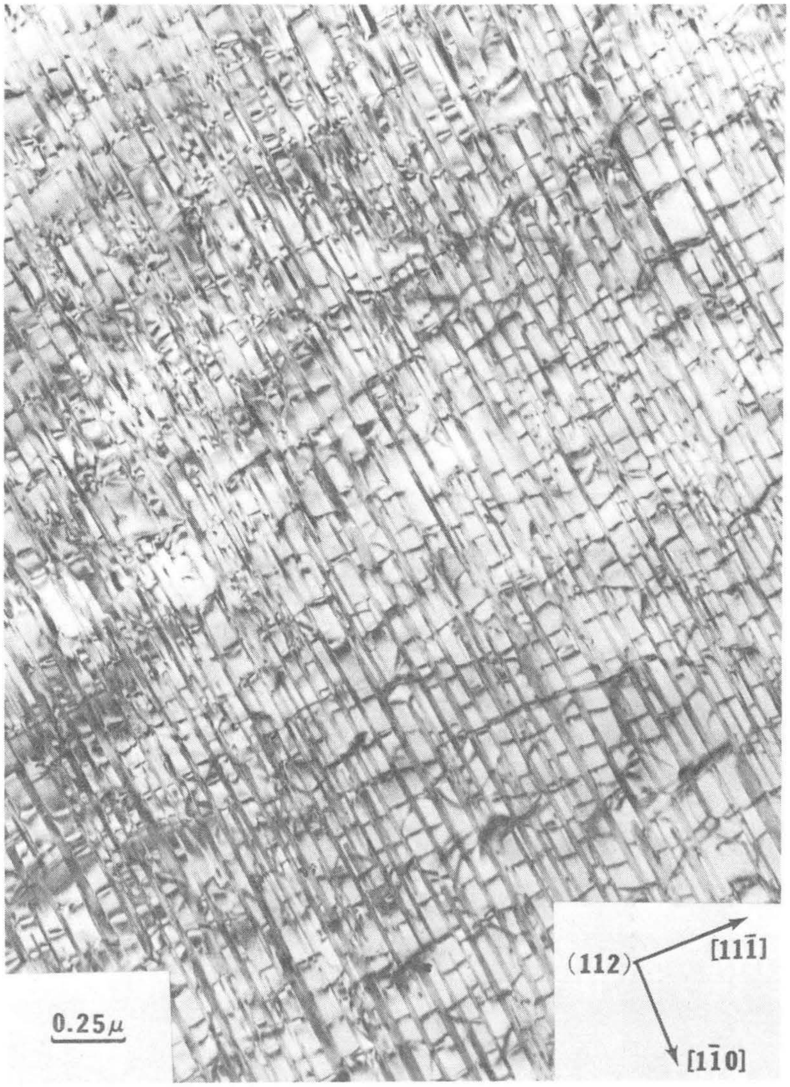

ZN-5654

Fig. 7

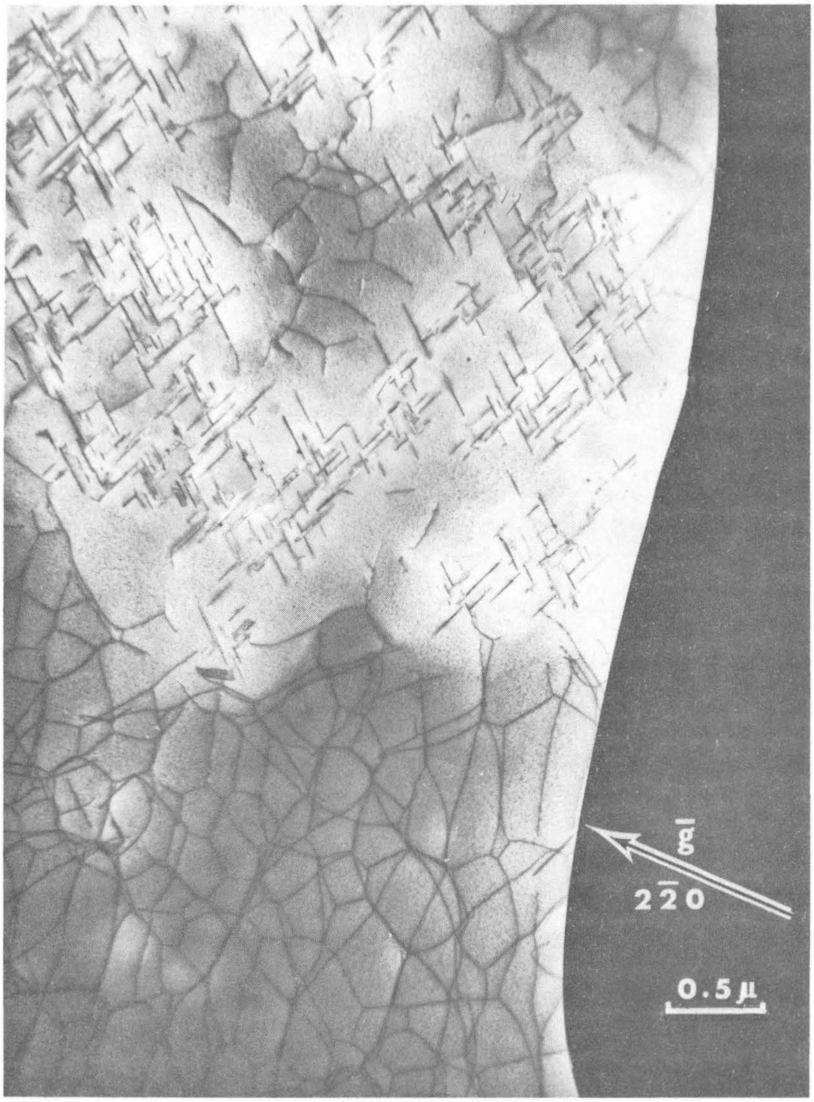

ZN-5664

Fig. 8

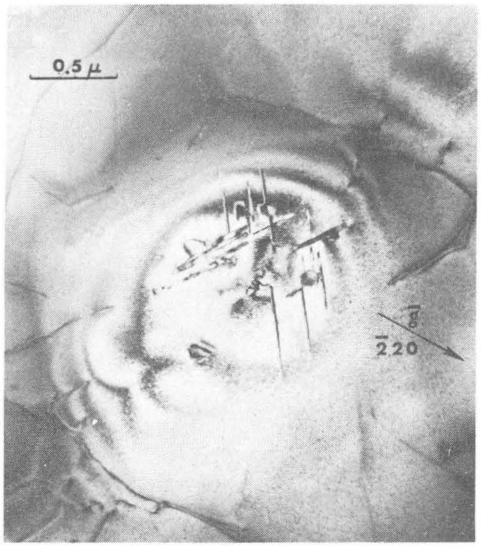

(a)

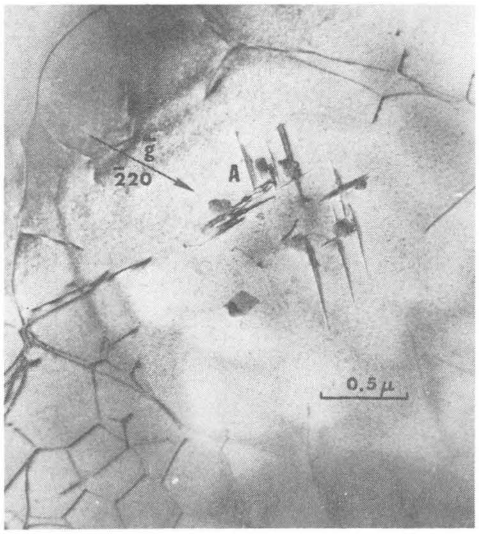

(b)

ZN-5655

Fig. 9

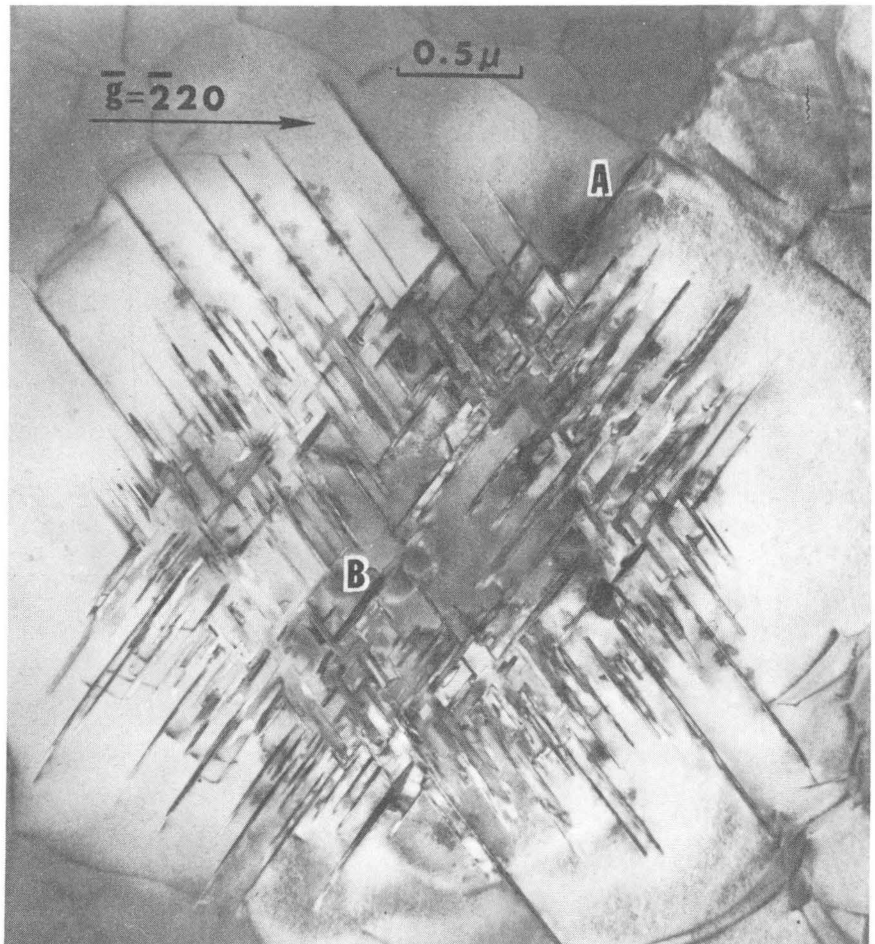

ZN-5658

Fig. 10

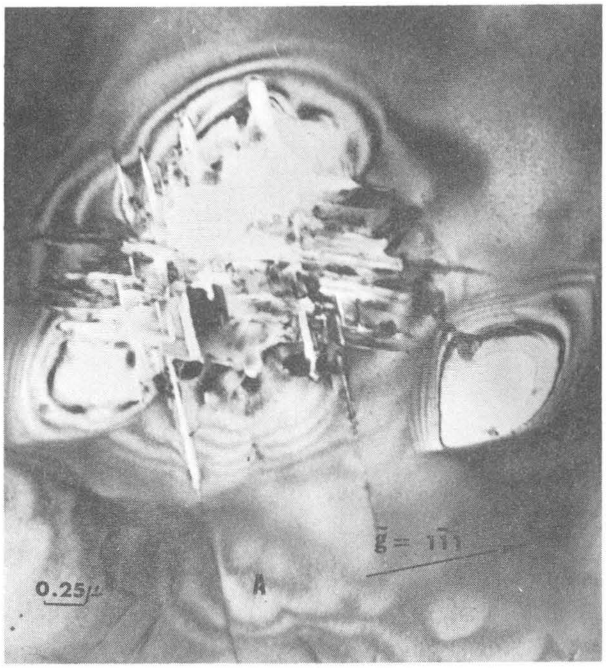

(a)

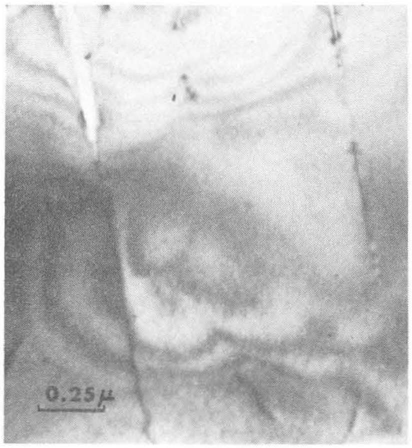

(b)

ZN-5656

Fig. 11

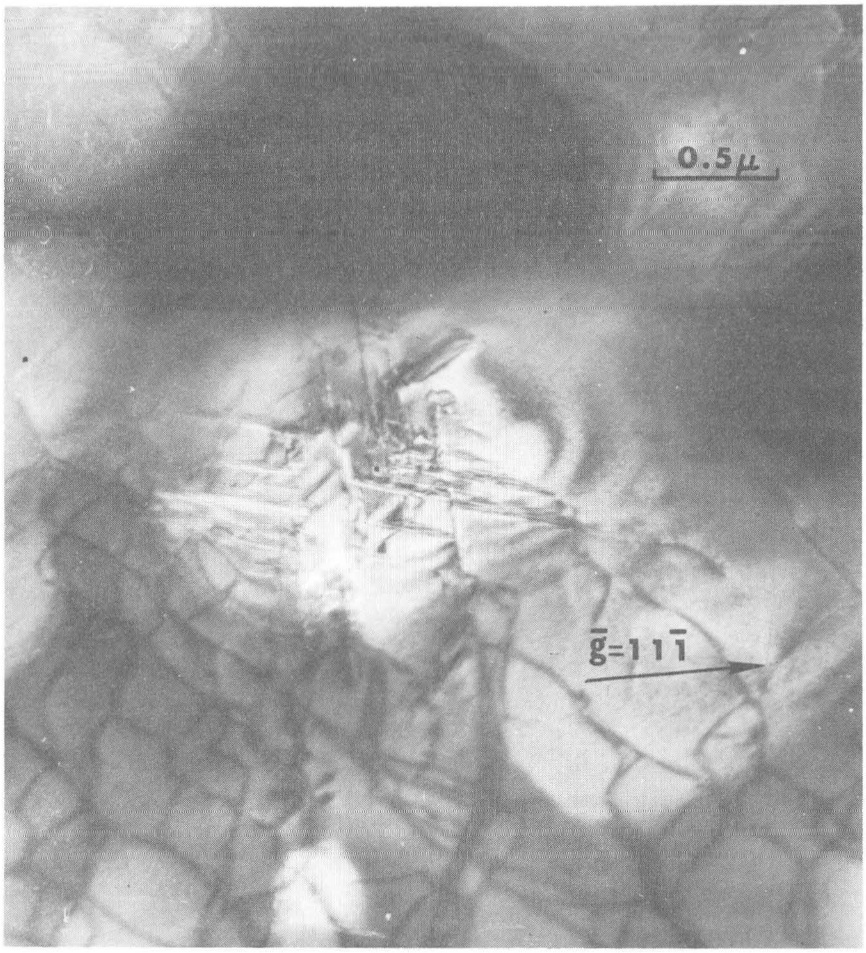

ZN-5659

Fig. 12

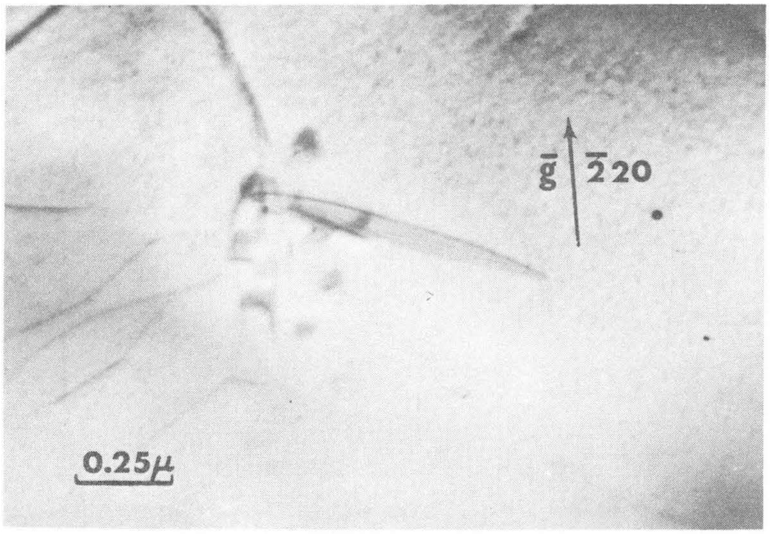

(a)

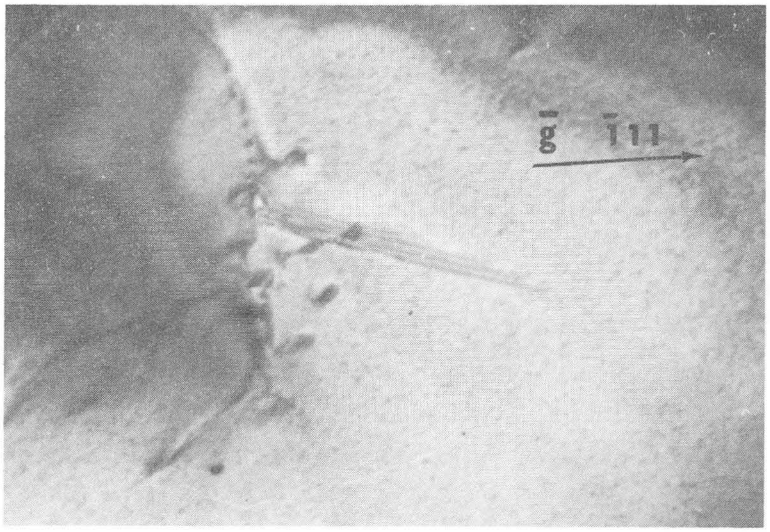

(b)

ZN-5657

Fig. 13

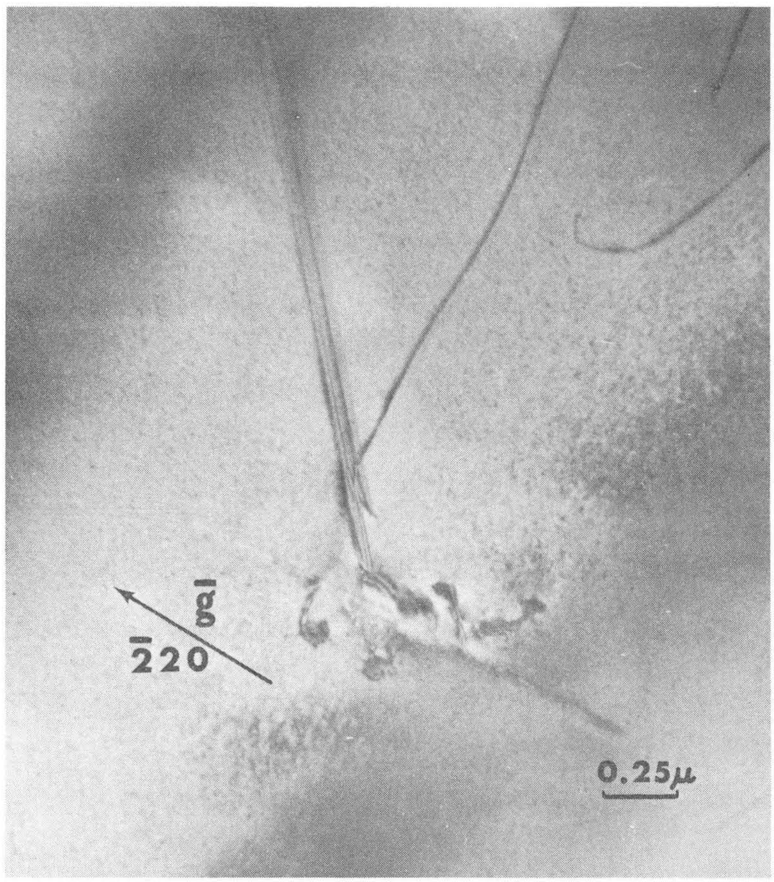

ZN-5665

Fig. 14